Receptor guanylyl cyclase C confers protection during oral *Salmonella* Typhimurium infection by attenuating ileal damage and enhancing cytokine and antimicrobial peptide production

Shamik Majumdar[a], Vishwas Mishra[b], Somesh Nandi[b], Mudabir Abdullah[b], Anaxee Barman[b], Abinaya Raghavan[a], Dipankar Nandi[a] and Sandhya S. Visweswariah[b#]

Department of Biochemistry[a], Department of Molecular Reproduction, Development and Genetics[b], Indian Institute of Science, Bangalore, India.

Running Head: Guanylyl cyclase C and *Salmonella* infection

Keywords: *Salmonella* Typhimurium; guanylyl cyclase C; guanylin; uroguanylin; thymic atrophy; goblet cell

Address correspondence to Sandhya S. Visweswariah : sandhya@iisc.ac.in

SM, VM and SN contributed equally to this work

Abstract

Non-typhoidal *Salmonella* disease contributes towards significant morbidity and mortality across the world. Host factors including IFN-γ, TNF-α and gut microbiota significantly influence the outcome of *Salmonella* pathogenesis. However, the entire repertoire of host protective mechanisms contributing to *Salmonella* pathogenicity is not completely appreciated. Here, we have investigated the roles of receptor guanylyl cyclase C (GC-C) that is predominantly expressed in the intestine, and regulates intestinal cell proliferation and fluid-ion homeostasis. Mice deficient in GC-C (*Gucy2c*$^{-/-}$) displayed accelerated mortality following infection via the oral route, in spite of possessing comparative systemic *Salmonella* infection burden. Survival following intra-peritoneal infection remained similar, indicating that GC-C offered protection via a gut-mediated response. Serum cortisol was higher in *Gucy2c*$^{-/-}$ mice, in comparison to wild type (*Gucy2c*$^{+/+}$) mice, and an increase in infection-induced thymic atrophy, with loss in immature CD4^{+}CD8^{+} double positive thymocytes, was observed. Accelerated and enhanced damage in the ileum, including submucosal edema, epithelial cell damage, focal tufting and distortion of villus architecture, was seen in *Gucy2c*$^{-/-}$ mice, concomitant with a larger number of ileal tissue-associated bacteria. Transcription of key mediators in *Salmonella*-induced inflammation (IL-22/IL-23/Reg3β) were altered in *Gucy2c*$^{-/-}$ mice. Downregulation of expression of GC-C and its endogenous ligands, guanylin and uroguanylin following infection in *Gucy2c*$^{+/+}$ mice was observed. In conclusion, our study suggests that receptor GC-C confers a survival advantage during gut-mediated *S.* Typhimurium pathogenesis, presumably by regulating *Salmonella*-effector mechanisms in a cGMP-dependent manner.

Introduction

42 Salmonellosis, the disease caused by the Gram-negative intracellular bacterium, *Salmonella*
43 manifests in humans as typhoid, paratyphoid fever, non-typhoidal septicemia or
44 gastroenteritis. Infection with *Salmonella* Typhi and Paratyphi serotypes are limited to
45 humans, and cause the systemic disease, typhoid fever. Infections with other serotypes, called
46 non-typhoidal *Salmonella*, result in enteritis and diarrhoea. *Salmonella* infects hosts orally via
47 contaminated food or water (1). Mice infection models are useful not only to study factors in
48 the pathogen that regulate disease progression, but also host factors that can modulate the
49 severity of response to *Salmonella* infection (2). In susceptible mouse strains, such as those
50 with defects in the gene encoding Slc11α1 (Nramp1), the bacterium traverses the distal ileum,
51 and mice develop systemic infection after colonizing the Peyer's patches, liver and spleen
52 (3).

53 Colonization of the mouse intestine is dependent on a number of factors, that include
54 commensal microflora, the gut mucosa and the gut-associated immune system. A number of
55 host factors such as IFN-γ (4), TNF-α (5, 6) and IL-22 modulate *Salmonella* pathogenesis (1).
56 These factors regulate the production of chemokines that recruit inflammatory cells to the site
57 of tissue damage and infection (7). In addition, it is conceivable that modulators of intestinal
58 epithelial cell function may also provide mechanisms to modulate *Salmonella* pathogenesis,
59 since the first point of contact for the pathogen is the epithelial cells that line the
60 gastrointestinal tract (8).

61 Receptor guanylyl cyclase C (GC-C) is a transmembrane receptor predominantly expressed
62 on the apical membrane of the intestinal enterocytes. It serves as a receptor for the
63 endogenous hormones, uroguanylin and guanylin (9, 10). Activation of GC-C upon ligand-
64 binding results in production of cGMP, which leads to protein kinase G II-dependent
65 activation of cystic fibrosis transmembrane conductance regulator (CFTR) and inhibition of
66 NHE3, the sodium–hydrogen exchanger 3. Consequently, activation of GC-C causes efflux of

67 chloride and CFTR-dependent bicarbonate secretion into the lumen and inhibition of sodium
68 absorption thus resulting in an osmotic gradient, finally leading to fluid accumulation in the
69 lumen. Hence, the major role of GC-C is in maintenance of fluid-ion homeostasis in the gut
70 (11). GC-C also serves as the receptor for the heat-stable enterotoxin (ST), the causative
71 agent of enterotoxigenic *Escherichia coli* (ETEC)-mediated diarrhoea in children and
72 traveller's diarrhoea (12, 13). Mice lacking GC-C are resistant to heat-stable enterotoxin-
73 induced fluid accumulation (13), and are reported to display higher susceptibility to dextran
74 sodium sulphate-induced colitis (14). Previously, we have demonstrated that mice lacking
75 GC-C show higher number of N-Methyl-N-nitrosourea-induced aberrant crypt foci (15),
76 indicating a role for GC-C in maintaining intestinal cell proliferation.

77 Mice deficient in GC-C i.e., *Gucy2c*$^{-/-}$ mice have been reported to possess a compromised gut
78 epithelial barrier which was attributed to the lower expression of tight junction proteins such
79 as occludin, claudin2 and claudin4 (14). *Citrobacter rodentium* (*C. rodentium*), an enteric
80 Gram-negative bacterium causes self-limiting infection in mice, and *Gucy2c*$^{-/-}$ mice are
81 reported to be more susceptible to infection by them (16). Here, we have studied the role of
82 GC-C as a host factor during *Salmonella*-mediated pathogenesis in mice. We find that in
83 contrast to expectations that a compromised gut barrier would lead to enhanced systemic
84 infection, the increased susceptibility of *Gucy2c*$^{-/-}$ mice to oral infection with *Salmonella*
85 Typhimurium (*S.* Typhimurium) was a result of increased bacterial load in the ileum and
86 altered cytokine production associated with increased ileal tissue damage.

87 **Results**

88 **Mice lacking GC-C display accelerated mortality during oral *S.* Typhimurium infection**

89 We infected C57BL/6 wild type (*Gucy2c*$^{+/+}$) and *Gucy2c*$^{-/-}$ mice orally with *S.* Typhimurium
90 and monitored their survival. We chose not to treat the mice with streptomycin (17), since we

91 were interested in an acute model of *S*. Typhimurium infection, without altering the existing
92 microbiota in these mice (18). Surprisingly, survival experiments revealed an increased
93 susceptibility of *Gucy2c*$^{-/-}$ mice to oral, but not intra-peritoneal, infection with *S*.
94 Typhimurium (Fig. 1a), indicating a role for GC-C in offering protection to gut-associated
95 infection. Median survival for *Gucy2c*$^{+/+}$ mice following oral infection was 112 h while it
96 was 80 h for *Gucy2c*$^{-/-}$ mice, and the difference was statistically significant (p = 0.006).
97 Interestingly, fecal excretion of bacteria was similar in *Gucy2c*$^{+/+}$ and *Gucy2c*$^{-/-}$ mice at early
98 stages of infection, as was the bacterial burden in organs such as the spleen, Peyer's patches
99 and liver on day 3 post infection (Fig. 1b, c). In agreement with earlier observations (19),
100 poor survival was correlated with a significant reduction in body weight of *Gucy2c*$^{-/-}$ mice on
101 day 3 (Fig. 1d).

102 Next, we monitored pro-inflammatory cytokines in the sera 3 days post oral infection, to
103 determine whether enhanced immune cell activation and inflammation was responsible for
104 the poor survival of *Gucy2c*$^{-/-}$ mice. As shown in Fig. 1e, while there was a tendency for an
105 increase in serum TNF-α and IL-6 levels on infection, the increase was not statistically
106 significant. IFN-γ levels were elevated on infection in both strains of mice, but there was no
107 difference between *Gucy2c*$^{+/+}$and *Gucy2c*$^{-/-}$ mice. Therefore, we conclude that an increase in
108 systemic infection or inflammation was not the cause for early death of *Gucy2c*$^{-/-}$ mice.

109 **Enhanced infection-induced thymic atrophy is observed in *Gucy2c*$^{-/-}$ mice**

110 We have previously reported that serum cortisol, a marker of general stress experienced by
111 the animal, is increased on *Salmonella* infection and contributes towards *S*. Typhimurium-
112 induced thymic atrophy in mice (20, 21). We monitored cortisol levels and observed an
113 increase in serum cortisol on infection. However, at 48 h, *Gucy2c*$^{-/-}$ mice showed higher
114 levels of circulating cortisol than that seen in *Gucy2c*$^{+/+}$ mice (Fig. 2a). Thymic atrophy was

115 observed in both *Gucy2c*$^{+/+}$ and *Gucy2c*$^{-/-}$ mice (Fig. 2b, c), but was more pronounced in
116 *Gucy2c*$^{-/-}$ mice, both at 48 and 96 h post infection (Fig. 2b). CD4 and CD8 cell surface
117 staining of isolated thymocytes revealed an increased depletion of CD4^{+}CD8^{+} thymocytes in
118 *Gucy2c*$^{-/-}$ mice post 96 hrs of infection (Fig. 2c).

119 **Increased epithelial damage in the small intestine is observed in *Gucy2c*$^{-/-}$ mice**

120 Results so far suggest that the protective effects of GC-C are mediated predominantly at the
121 level of the gastrointestinal tract, and could be initiated early during infection, thereby
122 resulting in gross systemic effects and earlier death in *Gucy2c*$^{+/+}$ mice. We therefore
123 monitored bacterial load in various regions of the gut following infection in both *Gucy2c*$^{+/+}$
124 and *Gucy2c*$^{-/-}$mice. Colony forming units (CFU) were enumerated on day 3 following
125 infection, at which time a few *Gucy2c*$^{-/-}$ mice had already succumbed. As shown in Fig. 3a,
126 while bacterial loads in the cecum and colon were similar in both the strains of mice, and an
127 almost 2-log order increase in bacteria was seen in the distal ileum.

128 We measured ileal damage and goblet cell number using Periodic Acid Schiff (PAS) staining
129 following paraformaldehyde fixation. Examination of small intestinal sections showed
130 marked histopathological differences between infected *Gucy2c*$^{+/+}$and *Gucy2c*$^{-/-}$ mice.
131 Infection resulted in more severe inflammation in the small intestine of *Gucy2c*$^{-/-}$ mice with
132 increased focal tufting and distortion of the crypt-villus architecture (Fig. 3b). A larger
133 number of dead cells were also observed in the lumen of the ileum at day 4 post infection.
134 PAS staining revealed a small but significant reduction in the number of goblet cells in
135 *Gucy2c*$^{-/-}$ mice even without infection. Also noteworthy is the intense staining of Paneth cells
136 in the crypts of both *Gucy2c*$^{+/+}$ and *Gucy2c*$^{-/-}$ mice following infection. Interestingly, the
137 number of goblet cells reduced in *Gucy2c*$^{+/+}$ mice, as has been reported earlier (17), while
138 there was a modest increase in *Gucy2c*$^{-/-}$ mice.

139 ***S*. Typhimurium infection downregulates the expression of GC-C and its ligands,**
140 **guanylin and uroguanylin**

141 Results so far indicate that signaling via GC-C protects the host during *Salmonella* infection,
142 by reducing the extent of tissue damage and colonization in the ileum. We therefore asked if
143 infection alters the expression of genes in the GC-C signaling pathway, which could be a
144 strategy used by *Salmonella* to increase its virulence in the host. We performed quantitative
145 real-time PCR analysis of cDNA prepared from the distal ileum of *Gucy2c*$^{+/+}$ mice on day 3
146 following oral infection and observed that the transcript levels of GC-C were significantly
147 reduced on infection (Fig. 4). The distal ileum is a region where both guanylin and
148 uroguanylin are expressed to comparable levels (22), and interestingly, transcript levels of
149 both the ligands were again reduced on infection in both *Gucy2c*$^{+/+}$ and *Gucy2c*$^{-/-}$ mice (Fig.
150 4). Therefore, turning off the GC-C signaling pathway may be beneficial to allow *Salmonella*
151 to colonize and establish infection.

152 Other genes downstream of GC-C did not show a change in expression levels (*Cftr*, *PkgII* and
153 *Pde5*). However, *Nhe3* transcripts were upregulated in both *Gucy2c*$^{+/+}$ and *Gucy2c*$^{-/-}$ mice.
154 Activation of GC-C results in cGMP-dependent phosphorylation of NHE3 that inhibits this
155 Na^+/H^+ exchanger (11, 23). Therefore, the downregulation of guanylin and uroguanylin
156 transcripts, coupled with increased expression of *Nhe3* would enhance Na^+ uptake by the
157 epithelial cells, possibly counteracting loss of this ion during *Salmonella*-induced diarrhoea.

158 **GC-C regulates transcription of cytokines and effectors during *Salmonella* infection**

159 Intestinal inflammation following *Salmonella* infection is a consequence of upregulation of
160 pro-inflammatory genes including *TNF-α*, *Il-1β*, *Il-22*, *Il-6*, *Ifn-γ* (24) and genes expressing
161 the C-type lectins *Reg3γ* and *Reg3β* (1). In agreement with enhanced bacterial loads in the
162 distal ileum, we saw a significant increase in TNF-α transcripts in *Gucy2c*$^{-/-}$ mice and

163 reduced IL-6 transcript levels following infection, in comparison to *Gucy2c*$^{+/+}$ mice (Fig. 5).
164 Interestingly, levels of IL-22 transcripts were significantly lower in *Gucy2c*$^{-/-}$ mice on
165 infection. This was correlated with little increase in IL-23 transcripts and its downstream
166 effector, Reg3β, in *Gucy2c*$^{-/-}$ mice . However, in agreement with higher bacterial load and
167 damage in the ileum, levels of lipocalin 2 transcripts were higher. A number of other
168 cytokines were similarly regulated in *Gucy2c*$^{+/+}$ and *Gucy2c*$^{-/-}$ mice, indicating a specific role
169 for GC-C signaling in modulating specific arms of the *Salmonella*-induced immune response.

170 **Reduced *Lactobacilli* in *Gucy2c*$^{-/-}$ mice could contribute to initial susceptibility of mice to**
171 ***Salmonella* infection**

172 The gut microbiota is known to influence infection progression by *Salmonella* (17, 18, 25,
173 26). We therefore monitored the major Phyla of bacteria present in the mouse gut, and also
174 *Lactobacillus sp* which has been reported to protect from *Salmonella* infection (25-28). We
175 prepared genomic DNA from stool samples from both *Gucy2c*$^{+/+}$ and *Gucy2c*$^{-/-}$ mice, and
176 performed real-time PCR using universal and Phyla specific primers for the 16S rRNA genes.
177 As shown in Fig. 6, while the major Phyla (*Bacteriodetes* and *Firmicutes*) were largely
178 unchanged in both strains of mice, *Lactobacillus sp* were significantly reduced. Since
179 *Lactobacilli* have been reported to attenuate the severity of salmonellosis in mice (25), we
180 propose that the initial environment of the gut of *Gucy2c*$^{-/-}$ mice could have also contributed
181 to initial infection and uptake of *S.* Typhimurium, culminating in the increased susceptibility
182 of *Gucy2c*$^{-/-}$ mice to infection.

183 **Discussion**

184 GC-C-mediated cGMP pathways are essential regulators of intestinal homeostasis, including
185 fluid-ion secretion and cell proliferation (23). The role of GC-C in diarrhea caused by
186 enterotoxigenic *E. coli* that produce heat-stable enterotoxins is well established, since GC-C

187 serves as the receptor for the toxin (11). However, the roles of GC-C, if any, during severe
188 enteric infections, have not been investigated. Here we have utilized the *S.* Typhimurium
189 infection model in mice which results in an acute, progressive and lethal infection, to study
190 the contribution of GC-C during *Salmonella* pathogenesis. Our results show that GC-C
191 provides a degree of protection to oral *S.* Typhimurium infection by reducing the extent of
192 ileal damage and modulating the levels of cytokines and antimicrobial peptides (AMPs) that
193 are known to combat *Salmonella (1, 24)* (Fig. 6b). Interestingly, the rapid mortality seen in
194 *Gucy2c*$^{-/-}$ mice was not result of increased systemic infection, since bacteria colonized
195 extraintestinal tissue to equivalent extents in both *Gucy2c*$^{+/+}$ and *Gucy2c*$^{-/-}$ mice.

196 Glucocorticoids (GCs) are steroid hormones which are secreted by the adrenal glands and
197 possess immunosuppressive properties. GCs are an indicator of stress (29) and are
198 upregulated during *S.* Typhimurium infection in mice (21). At 48 h post infection, serum
199 cortisol levels in *Gucy2c*$^{-/-}$ mice were significantly higher than that seen in *Gucy2c*$^{+/+}$ mice.
200 Thymic atrophy accompanies numerous infections and GCs contribute towards depletion of
201 the developing $CD4^{+}CD8^{+}$ immature thymocytes during infections by pathogens such as
202 *Listeria monocytogenes*, type A *Francisella tularensis*, *Trypanosoma cruzi* and *S.*
203 Typhimurium (20, 21). Since *Gucy2c*$^{-/-}$ mice displayed early elevated levels of serum cortisol
204 (Fig. 2a), infection-induced thymic atrophy in *Gucy2c*$^{-/-}$ mice was indeed observed to be
205 significantly higher than in *Gucy2c*$^{+/+}$ mice.

206 Higher circulating cortisol could be attributed to enhanced colonization and inflammation in
207 *Gucy2c*$^{-/-}$ mice, as evidenced by histopathology of the ileum. *S.* Typhimurium infection
208 results in inflammation of the cecum and colon, with lower inflammation seen in the ileum of
209 mice (30). Germ-free mice display higher ileal load than specific-pathogen-free mice when
210 administered with similar doses of *S.* Typhimurium (31). The higher colonization in the ileum
211 of *Gucy2c*$^{-/-}$ mice may be due to higher translocation or invasion of *Salmonella* in the gut of

212 these mice. Interestingly during Crohn's disease, selective inflammation in the terminal ileum
213 is observed. In addition, the standard therapy for inflammatory bowel disease (IBD) is
214 administration of corticosteroids, which facilitate immunosuppression (32). The elevated
215 levels of cortisol observed in *Gucy2c*$^{-/-}$ mice during infection (Fig. 2a) might be a
216 compensatory mechanism to reduce inflammation of the ileum.

217 *Salmonella* pathogenesis results in altered gene expression profile in the intestine (1). The
218 transcript levels of GC-C and its endogenous ligands, guanylin and uroguanylin were
219 downregulated upon infection in the ileum (Fig. 4). However, the transcript levels of other
220 downstream effectors of the GC-C pathway such as *PkgII, Cftr and Pde5* were not
221 differentially modulated post infection. NHE3 is an abundantly expressed Na^+/H^+ exchanger
222 in the intestine (11, 33). There was a significant increase in the expression of NHE3 upon
223 infection, which occurred independently of the presence of GC-C. The significant increase in
224 NHE3 transcript levels is counterintuitive, since there are reports of downregulation of NHE3
225 by pro-inflammatory cytokines such as IFN-γ and TNF-α and during conditions such as
226 EPEC infection and inflammatory bowel disease. However, NHE3 transcript levels are
227 increased by GCs (33). The increased cortisol amounts upon *Salmonella* infection may result
228 in the higher transcription of NHE3. Hitherto, mechanisms that lead to transcriptional
229 regulation of NHE3 upon *Salmonella* infection are unknown and warrant further
230 investigation.

231 There are only two reports so far of disruption of the GC-C signaling at both the receptor and
232 the ligand level, as we see here on *Salmonella* infection (Fig. 4, 6b). In ulcerative colitis
233 patients, a severity-dependent downregulation in expression of GC-C and its ligands,
234 guanylin and uroguanylin in the colonic mucosa is observed. GC-C and its ligands are also
235 downregulated in inflamed colonic IBD mucosa of patients, and in 2,4,6-Trinitrobenzene
236 sulphonic acid-induced colitis in rats (34). The significant downregulation of GC-C and its

237 ligands upon *Salmonella* infection could therefore occur as a consequence of inflammation
238 induced by infection.

239 *Salmonella* infection and invasion of the intestine induce inflammatory responses including
240 upregulation of pro-inflammatory cytokines (24). The induction of TNF-α in the
241 gastrointestinal tract during *Salmonella* infection is well known (5, 6). Low amounts of TNF-
242 α confer protection to mice towards *Salmonella* infection (35), while administration of higher
243 doses causes extensive histopathological damage, organ dysfunction and death within
244 minutes to hours due to respiratory arrest (36, 37). The upregulation of TNF-α has been
245 implicated to enhance inflammation and early pathological damage in the intestine during
246 *Salmonella* infection (5). *Gucy2c*$^{+/+}$ mice displayed a modest but non-significant increase in
247 transcript levels of TNF-α in the ileum, whereas a significant induction was observed in
248 *Gucy2c*$^{-/-}$ mice (Fig. 5). TNF-α also mediates the depletion of goblet cells during *S.*
249 Typhimurium infection in mice, as pre-treatment with anti-TNFα antibody restores the goblet
250 cell numbers and mucin profiles (6). We however see an increase in goblet cell numbers on
251 infection in the small intestine in *Gucy2c*$^{-/-}$ mice, suggesting a novel means of regulating
252 goblet cell number by GC-C not reported to date.

253 Neutrophils play major roles during acute inflammation and are the first leukocytes to be
254 recruited at the site of infection. Neutrophils can eradicate the pathogen by various
255 mechanisms and their recruitment to the inflamed site is crucial for bacterial clearance.
256 Cytokine production upon infection results in stimulation of epithelial cells to secrete CXC
257 chemokines which attract neutrophils to the site of inflammation (7). The expression of
258 various CXC ligands were upregulated in the ileum upon infection (Fig. 5). However, a
259 significant upregulation of CXCL2 was observed in *Gucy2c*$^{-/-}$ than in *Gucy2c*$^{+/+}$ mice (Fig.
260 5). CXCL2 is a pro-inflammatory, high affinity chemokine for the CXCR2 receptor present
261 on neutrophils (7). Higher expression of CXCL2 due to enhanced inflammation may result in

262 increased recruitment of neutrophils to the ileum of *Gucy2c*$^{-/-}$ mice, which was evident in the
263 ileal pathology (Fig. 3b).

264 A critical arm of the antimicrobial innate immune response is the production of epithelial
265 cell-derived AMPs. This antimicrobial response is mediated via the IL-22 cytokine, which
266 induces the expression of AMPs in the intestinal epithelial cells (1). IL-22 is produced by
267 leukocytes such as T helper type 17 (T_H17) cells in response to IL-23 produced by infected
268 dendritic cells and macrophages (38) and/or IL-6 produced by intestinal epithelial cells (39).
269 AMPs induced by IL-22 include REG3β, REG3γ, lipocalin 2 and calprotectin. REG3β and
270 REG3γ are bactericidal C-type lectins and eliminate Gram-positive bacteria (1, 40). Lipocalin
271 2 and calprotectin do not kill bacteria directly but starve them of metals which are essential
272 for their growth (1). This AMP response has been demonstrated to impart a growth advantage
273 to Gram-negative pathogens such as *Salmonella* over commensal bacteria (41). *Reg3γ*$^{-/-}$ and
274 *Reg3β*$^{-/-}$ mice are more susceptible to *Salmonella enteritidis* infection, implying a protective
275 role of these AMPs against this pathogen (42, 43). The lower infection-induced expression of
276 IL-6 and IL-23 in the ileum of *Gucy2c*$^{-/-}$ mice led to a lower expression of IL-22. This
277 reduced expression of IL-22 may affect the induction of AMPs in the epithelial cells, and
278 indeed, the transcript levels of Reg3β in *Gucy2c*$^{-/-}$ mice were found to be significantly lower
279 than in *Gucy2c*$^{+/+}$ mice upon infection, and may also partly account for the susceptibility of
280 these mice to *Salmonella* infection.

281 The gut microbiota is a critical determinant for susceptibility to various infectious pathogens
282 (44) including *S.* Typhimurium (17, 18, 25, 26). The gut microbiota can either promote
283 resistance to colonization of pathogens or assist and enhance its virulence (44). In our study,
284 there were no significant differences in the abundance of the major phyla i.e., *Bacteriordetes*,
285 *Firmicutes*, *Actinobacteria* and *Proteobacteria* in *Gucy2c*$^{+/+}$ and *Gucy2c*$^{-/-}$ mice (Fig. 6a).
286 However, a significant decrease in the abundance of *Lactobacillus* was observed in *Gucy2c*$^{-/-}$

287 mice which is in accordance with a previous observation made in these mice (16). Different
288 species and isolates of *Lactobacillus* have been shown to exert antagonistic activity on
289 Salmonella invasion and colonization (25-28). For example, *Lactobacillus acidophilus*
290 inhibits adhesion, invasion and dissemination of attenuated *S.* Typhimurium in BALB/c mice
291 (25). In vitro studies in human intestinal Caco-2 cells reveal that *Lactobacillus* mediates
292 *Salmonella*-induced intestinal inflammation via transforming growth factor β/MIR21
293 signaling pathway (26). The lower abundance of *Lactobacillus* might inherently predispose
294 *Gucy2c*$^{-/-}$ mice susceptible to *Salmonella* infection and may contribute to the higher degree of
295 translocation and epithelial damage in the ileum.

296 Microbiota dysbiosis has been reported in mice null for genes involved in fluid-ion
297 homeostasis of the gut (45, 46). It is possible that GC-C enhances growth and colonization of
298 *Lactobacillus* in the gut by providing and maintaining the luminal pH and/or electrolyte
299 distribution and balance. Further studies are required to comprehensively understand the role
300 of GC-C in regulating the distribution of gut microbiota.

301 In summary, we have studied the role of GC-C during *S.* Typhimurium infection in mice and
302 have identified GC-C as a crucial host factor that provides protection against gut-mediated
303 infection by *S.* Typhimurium. Our results summarized in Fig. 6b, indicate that *Salmonella*
304 infection results in downregulation of GC-C ligands and a modest but significant
305 downregulation of GC-C. Absence of GC-C in the gut modulates the innate immune response
306 to *Salmonella* and cytokine production, possibly affecting neutrophil migration in the distal
307 ileum. We speculate, therefore, that administration of GC-C ligand analogs may alleviate
308 *Salmonella*-mediated symptoms and pathology. Linaclotide is a FDA approved oral GC-C
309 ligand and is used in treatment of constipation and chronic idiopathic constipation. This drug
310 is effective against visceral pain associated with constipation predominant inflammatory
311 bowel syndrome (C-IBS) (47). Therefore, paradoxically, a target for a bacterial toxin that

312 causes diarrhoea may act as a therapeutic target for treatment and alleviation of *Salmonella*-
313 mediated intestinal symptoms and pathology.

314 **Materials and Methods**

315 **Bacterial cultures**

316 The *S.* Typhimurium NCTC 12023 strain was used for mice infections. A single isolated
317 colony of *S.* Typhimurium grown on a *Salmonella-Shigella* (SS) agar plate was used to grow
318 culture the pre-inoculum. The overnight pre-inoculum was used at 0.2% in 50 mL of Luria
319 broth and cultured for 3 hours at 37°C and 160 rpm to obtain a log phase culture. The
320 bacterial culture was washed and resuspended in sterile phosphate-buffered saline (PBS) and
321 used for infection (21).

322 **Mice**

323 *Gucy2c*$^{-/-}$ obtained from the Jackson laboratory, were backcrossed with C57BL/6 mice for
324 more than 10 generations. *Gucy2c*$^{+/+}$ and *Gucy2c*$^{-/-}$ mice were maintained as described
325 previously (15), and housed in a clean air facility. Temperature (22 ± 2°C) and humidity (55
326 ± 10%) were maintained with a 12 h light/dark cycle. Mice had access to laboratory chow
327 and water *ad libitum*. Mice aged 6-8 weeks of either sex, weighing 18-30 grams were used
328 for experiments.

329 **Ethics statement**

330 The experiments were performed in agreement with the Control and Supervision rules, 1998
331 of Ministry of Environment and Forest Act (Government of India) and the Institutional
332 Animal Ethics Committee of the Indian Institute of Science (IISc). *Gucy2c*$^{+/+}$ and *Gucy2c*$^{-/-}$
333 mice were bred and maintained at the Central Animal Facility of IISc (Registration number:
334 48/1999/CPCSEA, dated 1/3/1999). The experimental protocols were approved by the

335 'Committee for Purpose and Control and Supervision of Experiments on Animals'
336 (CPCSEA), permit number: CAF/Ethics/216/2011. The details of the national guidelines can
337 be found on: http://envfor.nic.in/division/committee-purpose-control-and-supervision-
338 experiments-animals-cpcsea (21).

339 **Mice infection**

340 The mice were infected with *S.* Typhimurium either orally or intra-peritoneally and survival
341 was monitored. For infections via the intra-peritoneal route, ~750 bacteria/mouse were
342 administered, while for oral infection, ~10^8 bacteria/mouse were used. The bacterial culture
343 was resuspended in PBS and 0.5 mL was administered either intraperitoneally or by oral
344 gavage.

345 Fresh fecal samples were collected following infection, weighed, homogenized in PBS and
346 the appropriate dilutions were plated on SS agar plates. For quantification of CFU burden in
347 organs, the mice were sacrificed at the indicated time points and the organs were harvested,
348 weighed and homogenized in PBS. Appropriate dilutions were plated on SS agar plates (20).

349 **Serum cytokines and cortisol estimation**

350 Serum TNF-α, IL-6 and IFN-γ were quantified using ELISA kits (eBioscience, USA), while
351 serum cortisol amounts were measured using the AccuBind ELISA kit (Monobind Inc., USA)
352 according to the manufacturer's instructions (21).

353 **Flow cytometric analysis of thymocytes**

354 On indicated days, uninfected and infected mice were sacrificed, thymi dissected and washed
355 in PBS. The organs were disrupted with a pair of forceps and the cell suspensions were
356 passed through a fine wire mesh to obtain a single cell suspension, and viability of the cells
357 was estimated by Trypan blue exclusion assay using a haemocytometer. Thymocytes were

358 stained for cell surface expression of CD4 and CD8 to estimate the major cell subpopulations.
359 Anti-mouse CD4-APC (17-0041-83) and anti-mouse CD8-PE (12-0081-85) were purchased
360 from eBioscience. Cells were incubated with fluorochrome-conjugated antibodies at 4°C for
361 45 mins. Subsequently, the cells were washed twice with PBS and fixed in 0.5%
362 paraformaldehyde. The cells were acquired on the FACSVerse™ flow cytometer (BD
363 Bioscience USA). Baseline instrument application and compensation settings were set using
364 unstained and single stained samples respectively. Single events were gated on the basis of
365 forward scatter-area versus forward scatter-height, while live events were gated on the basis
366 of forward scatter-area versus side scatter-area. These selections were considered to
367 exclusively analyse single live events. CD4 versus CD8 density plots were constructed for
368 thymocytes and the major cell populations were quantified. WinMDI and FlowJo (9.8.5)
369 software were used to plot and analyse the results (21).

370 **Histological analysis**

371 Histological analysis was performed on ileal sections, which were fixed in 4%
372 paraformaldehyde in PBS (pH 6.9) and Periodic Acid Schiff (PAS) staining was performed
373 (48). Briefly, following fixation, sections were dehydrated by serial immersion in increasing
374 concentrations of ethanol and finally in paraffin. The tissues were embedded in paraffin and 4
375 µm sections were obtained using a microtome (Leica Biosystems, Germany). The sections
376 were dewaxed and rehydrated by serial immersion in decreasing concentrations of ethanol.
377 Sections were stained with PAS (Avinash Chemicals, Bangalore, India) following the
378 manufacturer's instructions. The nuclei were subsequently stained with hematoxylin (Sigma-
379 Aldrich, USA). Sections were then dehydrated and mounted. The sections were observed
380 using an Olympus XI81 microscope (Olympus Corporation Tokyo, Japan).

381 **RNA isolation and quantitative real time PCR analysis**

382 A portion of the distal ileum was isolated and stored in TRI reagent (RNAiso Plus, TaKaRa).
383 The RNA was isolated using the QIAGEN RNeasy kit, according to manufacturer's protocol
384 and 4 μg of RNA was reverse transcribed to cDNA using Revert Aid reverse transcriptase
385 (Thermo-Scientific, USA). Real-time PCR was performed using SYBR® Premix Ex Taq™
386 (Tli RNaseH Plus) on a CFX96 Touch™ Real-Time PCR Detection System (BIO-RAD,
387 USA). Three housekeeping genes Glyceraldehyde 3-phosphate dehydrogenase (*Gapdh*),
388 TATA box binding protein (*Tbp*) and β-actin (*Actb*) were used for internal normalization
389 controls. Since all three genes showed equivalent results, *Gapdh* was used for subsequent
390 normalization of the real time PCR data. Data is expressed as $2^{-\Delta CT}$. The sequences of
391 primers used for quantitative real-time PCR were obtained from those validated at the
392 PrimerBank database and are available on request (49-51).

393 **Quantitative real-time PCR amplification of 16S sequences of fecal microbiota**

394 Bacterial DNA was isolated from fecal pellets using the QIAamp® DNA Stool Mini Kit
395 according to manufacturer's instructions. The abundance of total bacteria and specific
396 intestinal bacterial phylum, class and species was quantified by real-time PCR analysis by
397 SYBR® Premix Ex Taq™ (Tli RNaseH Plus) on a StepOnePlus real-time PCR machine
398 (Applied Biosystems, USA) using 16S primers published earlier (52, 53) . The efficiencies of
399 each primer were estimated (data not shown) and were found to be > 90%. Relative bacterial
400 abundance was determined using the ΔΔCT method by employing universal primers for 16s
401 rDNA for normalization (54).

402 **Statistical analysis**

403 All data was analysed using GraphPad Prism 7. The pooled results from independent
404 experiments are depicted as mean ± SD. Statistical significance among groups of mice were
405 determined using two-way ANOVA, with multiple comparisons, and FDR by the two-stage

406 linear step-up procedure of Benjamini, Krieger and Yekutieli. Students t-test with 95%
407 confidence interval was used for comparing abundance of microbiota in fecal samples.
408 Statistical significance between the mice survival curves were obtained by the Gehan-
409 Breslow-Wilcoxon test. The denoted p values are as follows: *p<0.05, **p<0.01,
410 ***p<0.001.

411 **Acknowledgements**

412 The authors acknowledge facilities provided by the Central Animal Facility at the Indian
413 Institute of Science for housing mice. Financial support from the Department of
414 Biotechnology, Government of India (SSV) is acknowledged, as well as support provided to
415 the Division of Biological Sciences in the form of a Grant-In-Aid by DBT. SSV is a JC Bose
416 National Fellow and support from the Department of Science and Technology, Government
417 of India, is acknowledged.

418

419 **References**

420 1. Santos RL, Raffatellu M, Bevins CL, Adams LG, Tukel C, Tsolis RM, Baumler AJ.
421 2009. Life in the inflamed intestine, Salmonella style. Trends Microbiol 17:498-506.
422 2. Hapfelmeier S, Hardt WD. 2005. A mouse model for S. typhimurium-induced
423 enterocolitis. Trends Microbiol 13:497-503.
424 3. Stecher B, Paesold G, Barthel M, Kremer M, Jantsch J, Stallmach T, Heikenwalder
425 M, Hardt WD. 2006. Chronic Salmonella enterica serovar Typhimurium-induced
426 colitis and cholangitis in streptomycin-pretreated Nramp1+/+ mice. Infect Immun
427 74:5047-57.

428 4. Bao S, Beagley KW, France MP, Shen J, Husband AJ. 2000. Interferon-gamma plays
429 a critical role in intestinal immunity against Salmonella typhimurium infection.
430 Immunology 99:464-72.
431 5. Arnold JW, Niesel DW, Annable CR, Hess CB, Asuncion M, Cho YJ, Peterson JW,
432 Klimpel GR. 1993. Tumor necrosis factor-alpha mediates the early pathology in
433 Salmonella infection of the gastrointestinal tract. Microb Pathog 14:217-27.
434 6. Arnold JW, Klimpel GR, Niesel DW. 1993. Tumor necrosis factor (TNF alpha)
435 regulates intestinal mucus production during salmonellosis. Cell Immunol 151:336-
436 44.
437 7. Sadik CD, Kim ND, Luster AD. 2011. Neutrophils cascading their way to
438 inflammation. Trends Immunol 32:452-60.
439 8. Zhou D, Galan J. 2001. Salmonella entry into host cells: the work in concert of type
440 III secreted effector proteins. Microbes Infect 3:1293-8.
441 9. Currie MG, Fok KF, Kato J, Moore RJ, Hamra FK, Duffin KL, Smith CE. 1992.
442 Guanylin: an endogenous activator of intestinal guanylate cyclase. Proc Natl Acad Sci
443 U S A 89:947-51.
444 10. Hamra FK, Forte LR, Eber SL, Pidhorodeckyj NV, Krause WJ, Freeman RH, Chin
445 DT, Tompkins JA, Fok KF, Smith CE, et al. 1993. Uroguanylin: structure and activity
446 of a second endogenous peptide that stimulates intestinal guanylate cyclase. Proc Natl
447 Acad Sci U S A 90:10464-8.
448 11. Basu N, Arshad N, Visweswariah SS. 2010. Receptor guanylyl cyclase C (GC-C):
449 regulation and signal transduction. Mol Cell Biochem 334:67-80.
450 12. Schulz S, Green CK, Yuen PS, Garbers DL. 1990. Guanylyl cyclase is a heat-stable
451 enterotoxin receptor. Cell 63:941-8.

452 13. Schulz S, Lopez MJ, Kuhn M, Garbers DL. 1997. Disruption of the guanylyl cyclase-
453 C gene leads to a paradoxical phenotype of viable but heat-stable enterotoxin-resistant
454 mice. J Clin Invest 100:1590-5.
455 14. Lin JE, Snook AE, Li P, Stoecker BA, Kim GW, Magee MS, Garcia AV, Valentino
456 MA, Hyslop T, Schulz S, Waldman SA. 2012. GUCY2C opposes systemic genotoxic
457 tumorigenesis by regulating AKT-dependent intestinal barrier integrity. PLoS One
458 7:e31686.
459 15. Basu N, Saha S, Khan I, Ramachandra SG, Visweswariah SS. 2014. Intestinal cell
460 proliferation and senescence are regulated by receptor guanylyl cyclase C and p21. J
461 Biol Chem 289:581-93.
462 16. Mann EA, Harmel-Laws E, Cohen MB, Steinbrecher KA. 2013. Guanylate cyclase C
463 limits systemic dissemination of a murine enteric pathogen. BMC Gastroenterol
464 13:135.
465 17. Barthel M, Hapfelmeier S, Quintanilla-Martinez L, Kremer M, Rohde M, Hogardt M,
466 Pfeffer K, Russmann H, Hardt WD. 2003. Pretreatment of mice with streptomycin
467 provides a Salmonella enterica serovar Typhimurium colitis model that allows
468 analysis of both pathogen and host. Infect Immun 71:2839-58.
469 18. Sekirov I, Tam NM, Jogova M, Robertson ML, Li Y, Lupp C, Finlay BB. 2008.
470 Antibiotic-induced perturbations of the intestinal microbiota alter host susceptibility
471 to enteric infection. Infect Immun 76:4726-36.
472 19. Ren Z, Gay R, Thomas A, Pae M, Wu D, Logsdon L, Mecsas J, Meydani SN. 2009.
473 Effect of age on susceptibility to Salmonella Typhimurium infection in C57BL/6
474 mice. J Med Microbiol 58:1559-67.
475 20. Deobagkar-Lele M, Chacko SK, Victor ES, Kadthur JC, Nandi D. 2013. Interferon-
476 gamma- and glucocorticoid-mediated pathways synergize to enhance death of CD4(+)

477 CD8(+) thymocytes during Salmonella enterica serovar Typhimurium infection.
478 Immunology 138:307-21.
479 21. Majumdar S, Deobagkar-Lele M, Adiga V, Raghavan A, Wadhwa N, Ahmed SM,
480 Rananaware SR, Chakraborty S, Joy O, Nandi D. 2017. Differential susceptibility and
481 maturation of thymocyte subsets during Salmonella Typhimurium infection: insights
482 on the roles of glucocorticoids and Interferon-gamma. Sci Rep 7:40793.
483 22. Ikpa PT, Sleddens HF, Steinbrecher KA, Peppelenbosch MP, de Jonge HR, Smits R,
484 Bijvelds MJ. 2016. Guanylin and uroguanylin are produced by mouse intestinal
485 epithelial cells of columnar and secretory lineage. Histochem Cell Biol 146:445-55.
486 23. Arshad N, Visweswariah SS. 2012. The multiple and enigmatic roles of guanylyl
487 cyclase C in intestinal homeostasis. FEBS Lett 586:2835-40.
488 24. LaRock DL, Chaudhary A, Miller SI. 2015. Salmonellae interactions with host
489 processes. Nat Rev Microbiol 13:191-205.
490 25. Nakazato G, Paganelli F, Lago J, Aoki F, Mobilon C, Brocchi M, Stehling E, Silveira
491 W. 2011. Lactobacillus acidophilus decreases Salmonella Typhimurium invasion in
492 vivo. Journal of Food Safety 31:284-289.
493 26. Huang IF, Lin IC, Liu PF, Cheng MF, Liu YC, Hsieh YD, Chen JJ, Chen CL, Chang
494 HW, Shu CW. 2015. Lactobacillus acidophilus attenuates Salmonella-induced
495 intestinal inflammation via TGF-beta signaling. BMC Microbiol 15:203.
496 27. Abdel-Daim A, Hassouna N, Hafez M, Ashor MS, Aboulwafa MM. 2013.
497 Antagonistic activity of Lactobacillus isolates against Salmonella typhi in vitro.
498 Biomed Res Int 2013:680605.
499 28. Coconnier MH, Lievin V, Lorrot M, Servin AL. 2000. Antagonistic activity of
500 Lactobacillus acidophilus LB against intracellular Salmonella enterica serovar

501 Typhimurium infecting human enterocyte-like Caco-2/TC-7 cells. Appl Environ
502 Microbiol 66:1152-7.
503 29. Nicolaides NC, Kyratzi E, Lamprokostopoulou A, Chrousos GP, Charmandari E.
504 2015. Stress, the stress system and the role of glucocorticoids.
505 Neuroimmunomodulation 22:6-19.
506 30. Tannock GW, Blumershine RV, Savage DC. 1975. Association of Salmonella
507 typhimurium with, and its invasion of, the ileal mucosa in mice. Infect Immun
508 11:365-70.
509 31. Stecher B, Macpherson AJ, Hapfelmeier S, Kremer M, Stallmach T, Hardt WD. 2005.
510 Comparison of Salmonella enterica serovar Typhimurium colitis in germfree mice and
511 mice pretreated with streptomycin. Infect Immun 73:3228-41.
512 32. Cominelli F, Arseneau KO, Rodriguez-Palacios A, Pizarro TT. 2017. Uncovering
513 Pathogenic Mechanisms of Inflammatory Bowel Disease Using Mouse Models of
514 Crohn's Disease-Like Ileitis: What is the Right Model? Cell Mol Gastroenterol
515 Hepatol 4:19-32.
516 33. He P, Yun CC. 2010. Mechanisms of the regulation of the intestinal Na+/H+
517 exchanger NHE3. J Biomed Biotechnol 2010:238080.
518 34. Pattison AM, Merlino DJ, Blomain ES, Waldman SA. 2016. Guanylyl cyclase C
519 signaling axis and colon cancer prevention. World J Gastroenterol 22:8070-7.
520 35. Nakano Y, Onozuka K, Terada Y, Shinomiya H, Nakano M. 1990. Protective effect
521 of recombinant tumor necrosis factor-alpha in murine salmonellosis. J Immunol
522 144:1935-41.
523 36. Tracey KJ, Beutler B, Lowry SF, Merryweather J, Wolpe S, Milsark IW, Hariri RJ,
524 Fahey TJ, 3rd, Zentella A, Albert JD, et al. 1986. Shock and tissue injury induced by
525 recombinant human cachectin. Science 234:470-4.

526 37. Beutler B, Grau GE. 1993. Tumor necrosis factor in the pathogenesis of infectious
527 diseases. Crit Care Med 21:S423-35.
528 38. Zheng Y, Danilenko DM, Valdez P, Kasman I, Eastham-Anderson J, Wu J, Ouyang
529 W. 2007. Interleukin-22, a T(H)17 cytokine, mediates IL-23-induced dermal
530 inflammation and acanthosis. Nature 445:648-51.
531 39. Powell N, Lo JW, Biancheri P, Vossenkamper A, Pantazi E, Walker AW, Stolarczyk
532 E, Ammoscato F, Goldberg R, Scott P, Canavan JB, Perucha E, Garrido-Mesa N,
533 Irving PM, Sanderson JD, Hayee B, Howard JK, Parkhill J, MacDonald TT, Lord
534 GM. 2015. Interleukin 6 Increases Production of Cytokines by Colonic Innate
535 Lymphoid Cells in Mice and Patients With Chronic Intestinal Inflammation.
536 Gastroenterology 149:456-67 e15.
537 40. Vaishnava S, Yamamoto M, Severson KM, Ruhn KA, Yu X, Koren O, Ley R,
538 Wakeland EK, Hooper LV. 2011. The antibacterial lectin RegIIIgamma promotes the
539 spatial segregation of microbiota and host in the intestine. Science 334:255-8.
540 41. Behnsen J, Jellbauer S, Wong CP, Edwards RA, George MD, Ouyang W, Raffatellu
541 M. 2014. The cytokine IL-22 promotes pathogen colonization by suppressing related
542 commensal bacteria. Immunity 40:262-73.
543 42. van Ampting MT, Loonen LM, Schonewille AJ, Konings I, Vink C, Iovanna J,
544 Chamaillard M, Dekker J, van der Meer R, Wells JM. 2012. Intestinally secreted C-
545 type lectin Reg3b attenuates salmonellosis but not listeriosis in mice. Infection and
546 immunity 80:1115-1120.
547 43. Loonen LM, Stolte EH, Jaklofsky MT, Meijerink M, Dekker J, van Baarlen P, Wells
548 JM. 2014. REG3gamma-deficient mice have altered mucus distribution and increased
549 mucosal inflammatory responses to the microbiota and enteric pathogens in the ileum.
550 Mucosal Immunol 7:939-47.

551 44. Bäumler AJ, Sperandio V. 2016. Interactions between the microbiota and pathogenic
552 bacteria in the gut. Nature 535:85-93.
553 45. Larmonier CB, Laubitz D, Hill FM, Shehab KW, Lipinski L, Midura-Kiela MT,
554 McFadden RM, Ramalingam R, Hassan KA, Golebiewski M, Besselsen DG, Ghishan
555 FK, Kiela PR. 2013. Reduced colonic microbial diversity is associated with colitis in
556 NHE3-deficient mice. Am J Physiol Gastrointest Liver Physiol 305:G667-77.
557 46. Norkina O, Burnett TG, De Lisle RC. 2004. Bacterial overgrowth in the cystic
558 fibrosis transmembrane conductance regulator null mouse small intestine. Infect
559 Immun 72:6040-9.
560 47. Castro J, Harrington AM, Hughes PA, Martin CM, Ge P, Shea CM, Jin H, Jacobson
561 S, Hannig G, Mann E, Cohen MB, MacDougall JE, Lavins BJ, Kurtz CB, Silos-
562 Santiago I, Johnston JM, Currie MG, Blackshaw LA, Brierley SM. 2013. Linaclotide
563 inhibits colonic nociceptors and relieves abdominal pain via guanylate cyclase-C and
564 extracellular cyclic guanosine 3',5'-monophosphate. Gastroenterology 145:1334-46
565 e1-11.
566 48. Crepin VF, Collins JW, Habibzay M, Frankel G. 2016. Citrobacter rodentium mouse
567 model of bacterial infection. Nat Protoc 11:1851-76.
568 49. Wang X, Seed B. 2003. A PCR primer bank for quantitative gene expression analysis.
569 Nucleic Acids Res 31:e154.
570 50. Spandidos A, Wang X, Wang H, Dragnev S, Thurber T, Seed B. 2008. A
571 comprehensive collection of experimentally validated primers for Polymerase Chain
572 Reaction quantitation of murine transcript abundance. BMC Genomics 9:633.
573 51. Spandidos A, Wang X, Wang H, Seed B. 2010. PrimerBank: a resource of human and
574 mouse PCR primer pairs for gene expression detection and quantification. Nucleic
575 Acids Res 38:D792-9.

576 52. Yang Y-W, Chen M-K, Yang B-Y, Huang X-J, Zhang X-R, He L-Q, Zhang J, Hua Z-
577 C. 2015. Use of 16S rRNA gene-targeted group-specific primers for real-time PCR
578 analysis of predominant bacteria in mouse feces. Applied and environmental
579 microbiology 81:6749-6756.
580 53. Clifford RJ, Milillo M, Prestwood J, Quintero R, Zurawski DV, Kwak YI, Waterman
581 PE, Lesho EP, Mc Gann P. 2012. Detection of bacterial 16S rRNA and identification
582 of four clinically important bacteria by real-time PCR. PloS one 7:e48558.
583 54. Feng Y, Gong J, Yu H, Jin Y, Zhu J, Han Y. 2010. Identification of changes in the
584 composition of ileal bacterial microbiota of broiler chickens infected with Clostridium
585 perfringens. Vet Microbiol 140:116-21.

586

587 **Legends to Figures**

588 **Figure 1: *Gucy2c*$^{-/-}$ mice display accelerated mortality during oral infection with *S.***
589 **Typhimurium.** (a) *Gucy2c*$^{+/+}$ and *Gucy2c*$^{-/-}$ mice were infected with *S*. Typhimuirum either
590 orally or intra-peritoneally. The mice were monitored for survival at 8 h intervals. Survival
591 curves for oral and intra-peritoneal infection were obtained from independent experiments
592 containing a total of 10-11 mice. (b) Mice (*Gucy2c*$^{+/+}$, black circles; *Gucy2c*$^{-/-}$, grey circles)
593 were orally infected with *S*. Typhimurium and the bacterial load in the feces on day 1 and 2
594 following infection were estimated. Data show values for individual mice, with error bars
595 showing the mean ± SD. (c) Infected mice were sacrificed on day 3, tissues harvested and
596 bacterial burden in the spleen, Peyer's patches and liver was estimated. Data show values for
597 individual mice, with error bars showing the mean ± SD. (d) Mice were weighed prior to oral
598 infection and 3 days post infection. (e) Serum was collected from uninfected and infected
599 mice and levels of TNF-α, IFN-γ and IL-6 were measured by ELISA. In panels b-e, the data
600 are depicted as mean ± SD of 3-7 mice per group. Statistical significance among the
601 experimental groups in all panels was analysed using two-way ANOVA, *$p \leq 0.05$ and ns: not
602 significant.

603

604 **Figure 2. Early rise in serum cortisol amounts and increased infection-induced thymic**
605 **atrophy is observed in *Gucy2c*$^{-/-}$ mice.** (a) *Gucy2c*$^{+/+}$ and *Gucy2c*$^{-/-}$ mice were orally
606 infected with *S*. Typhimurium. At the indicated time points, uninfected (-St) and infected
607 (+St) mice were sacrificed and serum cortisol levels were measured by ELISA. Data show
608 values for individual mice, with error bars showing the mean ± SD. (b) Viable cells from
609 harvested thymi were quantified by Trypan blue exclusion assay using a haemocytometer. (c)
610 The thymocytes from uninfected (-St) and mice post 96 h of infection (+St) were stained for

611 cell surface expression of CD4 and CD8 and the density plots were constructed to quantify
612 the percentages of the major cell populations. Data are depicted as mean ± SEM of 5-8 mice
613 per group. In all panels, experimental groups were analysed for statistical significance using
614 two-way ANOVA, $*p \leq 0.05$, $***p \leq 0.001$ and $****p \leq 0.0001$. Green bars indicate
615 differences that were statistically significant between *Gucy2c*$^{+/+}$ (black circles) and *Gucy2c*$^{-/-}$
616 (grey circles) mice.

617

618 **Figure 3: *Gucy2c*$^{-/-}$ mice show increased bacterial colonization and intestinal damage.**
619 Infected *Gucy2c*$^{+/+}$ (black circles) and *Gucy2c*$^{-/-}$ (grey circles) mice were sacrificed 3 days
620 post oral *S*. Typhimurium infection. (a) Bacterial load in the ileum, cecum and colon was
621 estimated. Values represent individual mice, and lines show the mean ± SD. (b) Periodic
622 Acid Schiff (PAS) staining was performed on formalin fixed ileal tissue sections obtained
623 from uninfected (-St) and infected (+St) on day 3 and 4 following infection. One
624 representative ileal tissue section from each experimental group containing 3-4 mice is
625 depicted, and the scale bars measure 100 µm. Arrow shows a large number of apoptic cells in
626 the lumen of *Gucy2c*$^{-/-}$ mice. (c) The number of goblet cells was quantified in individual,
627 clearly identifiable, villi in each section from uninfected (–St; black circles) and infected
628 (+St; red circles) mice. Data shown is from individual villi across a section, and lines indicate
629 the mean ± SD. Statistical analysis was performed by two-way ANOVA and $*p \leq 0.05$.

630

631 **Figure 4. *S.* Typhimurium infection regulates expression of genes in the GC-C signaling**
632 **pathway.** RNA was prepared from ileal tissue of uninfected (-St) and infected (+St) mice on
633 day 3 following oral infection. Quantitative real-time PCR analysis was performed to
634 estimate the transcript levels of *Gucy2c*, *Guca2a, Guca2b, PkgII, Pde5, Nhe3 and Cftr*. The

635 data are depicted as values for individual mice, and lines represent the mean ± SD. Two-way
636 ANOVA was used to analyse for statistical significance among the experimental groups, *$p \leq$
637 0.05, **$p \leq 0.01$, ***$p \leq 0.001$ and ns: not significant.

638

639 **Figure 5. *Gucy2c*$^{-/-}$ mice show reduced transcript levels of IL-23/IL-22 in the ileum**
640 **following infection.** Orally infected *Gucy2c*$^{+/+}$ and *Gucy2c*$^{-/-}$ mice were sacrificed 3 days
641 post infection (+St) along with the control uninfected mice (-St). RNA was isolated from the
642 harvested ileal tissues and quantitative real-time PCR analysis was performed to estimate the
643 transcript levels of *Tnf-α, Il-1b, Il-6, Il-8, Il-22, Il-23, Ifn-γ, Il-4, Cxcl-1, Cxcl-2, Cxcl-9, Cxcl-*
644 *10, Lcn 2, Reg3β* and *Reg3γ.* The data shown are from individual mice and lines depict the
645 mean ± SD. The experimental groups were analysed for statistical significance using two-
646 way ANOVA, *$p \leq 0.05$, **$p \leq 0.01$, ***$p \leq 0.001$ and ns: not significant. Green bars
647 represent values which differed significantly between *Gucy2c*$^{+/+}$ and *Gucy2c*$^{-/-}$ mice.

648

649 **Figure 6. Abundance of major microbial phyla in *Gucy2c*$^{+/+}$ and *Gucy2c*$^{-/-}$ mice.** (a) Fecal
650 pellets from uninfected *Gucy2c*$^{+/+}$ and *Gucy2c*$^{-/-}$ mice were collected and the bacterial DNA
651 was isolated from the samples. Quantitative real-time PCR was performed to analyse levels
652 of gut microbiota using Phyla specific primers, normalized to universal 16S primers. Values
653 shown represent individual mice and lines show the mean ± SD. Statistical analysis was
654 performed using non-parametric Mann-Whitney *U* test, **$p \leq 0.01$. (b) The IL23/IL22 arm of
655 the innate immune response during *Salmonella* infection is regulated by GC-C. Post oral
656 infection in mice, *Salmonella* competes with the commensal *Lactobacillus* to invade the
657 epithelial and dendritic cells of the gut. *Salmonella* downregulates the expression of the GC-
658 C receptor and its endogenous ligands, guanylin and urouanylin. Probable interaction of GC-

659 C with dendritic cells and macrophages along with IL-6 upregulation leads to induction of IL-
660 23 expression, which activates the TH17 cells to express the cytokine IL-22, which in turn
661 induces the expression of the AMP, Reg3β, in epithelial cells.

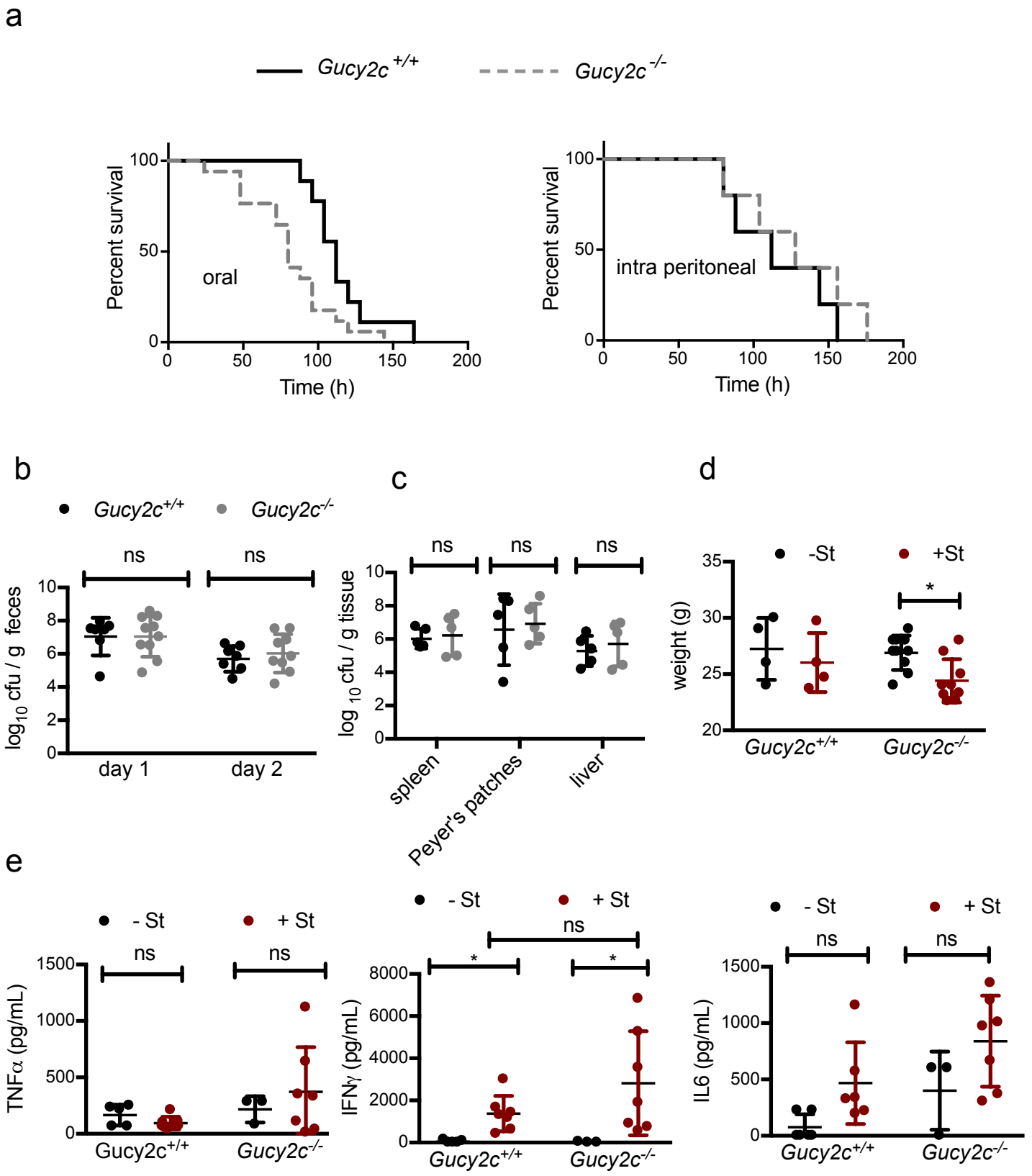
a
Gucy2c +/+
Gucy2c -/-
Percent survival
oral
Time (h)
intra peritoneal
b
Gucy2c+/+
Gucy2c-/-
ns
log10 cfu / g feces
day 1
day 2
c
log 10 cfu / g tissue
spleen
Peyer's patches
liver
d
-St
+St
weight (g)
*
e
- St
+ St
TNFα (pg/mL)
IFNγ (pg/mL)
IL6 (pg/mL)

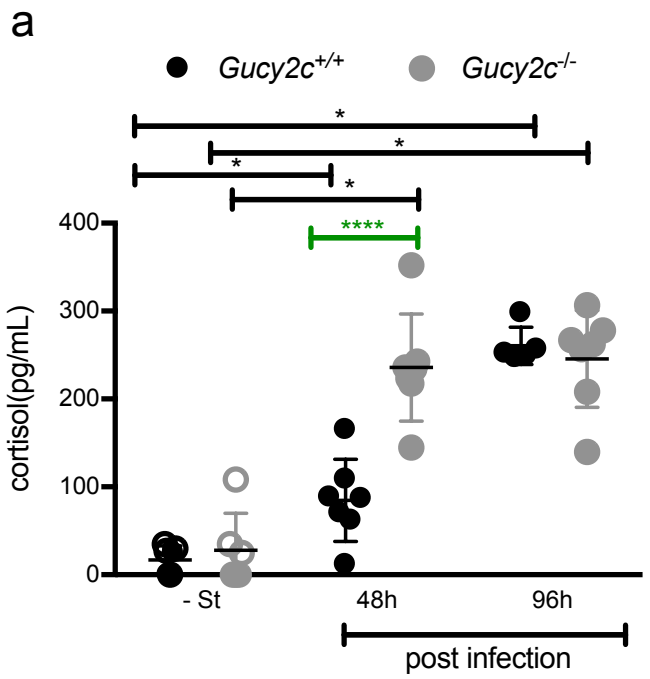
a
Gucy2c+/+
Gucy2c-/-
cortisol(pg/mL)
400
300
200
100
0
- St
48h
96h
post infection
*
*
*
*
****

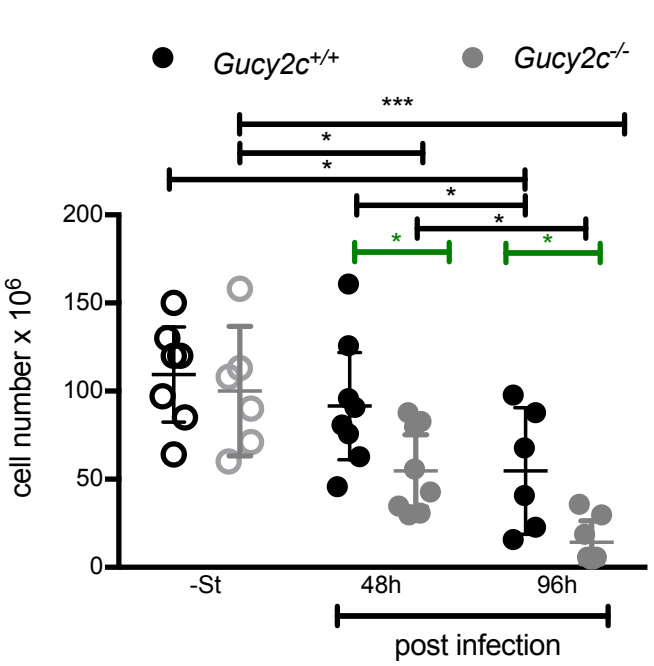
b
Gucy2c+/+
Gucy2c-/-
cell number x 10^6
200
150
100
50
0
-St
48h
96h
post infection
***
*
*
*
*
*
*
*

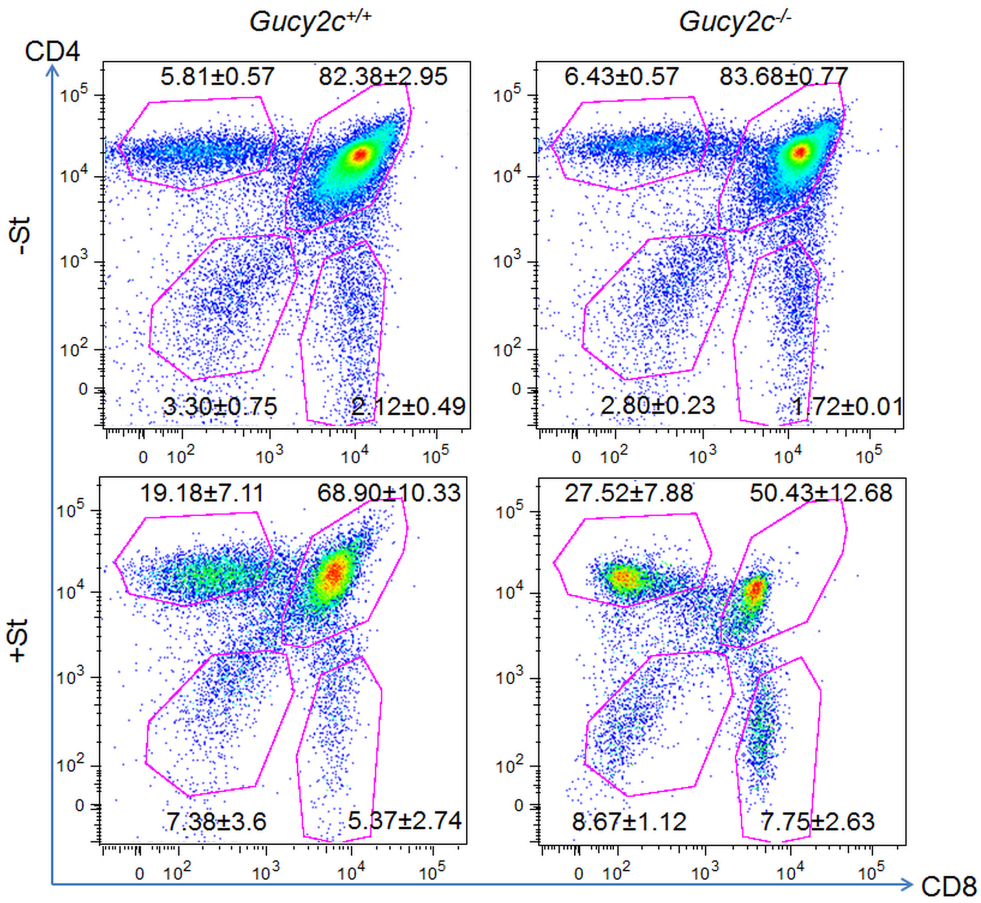
c
Gucy2c+/+
Gucy2c-/-
CD4
CD8
-St
+St
5.81±0.57
82.38±2.95
3.30±0.75
2.12±0.49
6.43±0.57
83.68±0.77
2.80±0.23
1.72±0.01
19.18±7.11
68.90±10.33
7.38±3.6
5.37±2.74
27.52±7.88
50.43±12.68
8.67±1.12
7.75±2.63

a

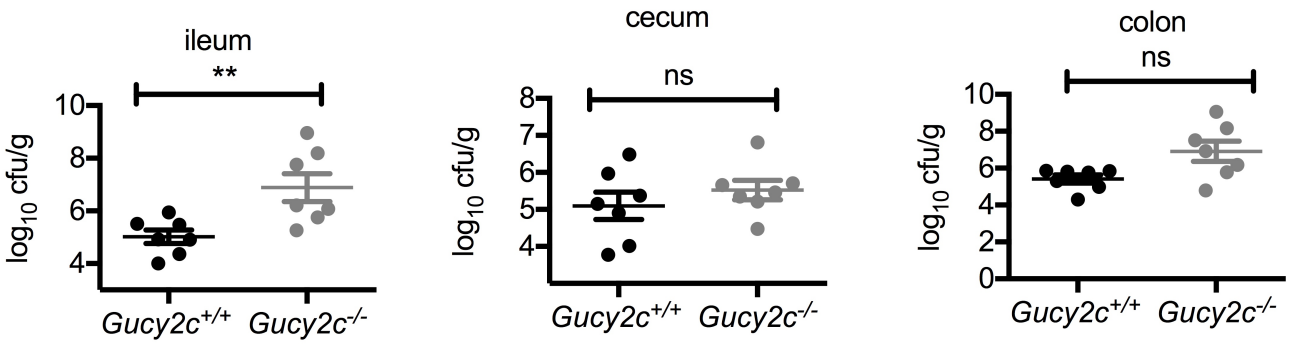
ileum
**
log10 cfu/g
10
8
6
4
Gucy2c+/+
Gucy2c-/-
cecum
ns
log10 cfu/g
8
7
6
5
4
Gucy2c+/+
Gucy2c-/-
colon
ns
log10 cfu/g
10
8
6
4
2
0
Gucy2c+/+
Gucy2c-/-

b

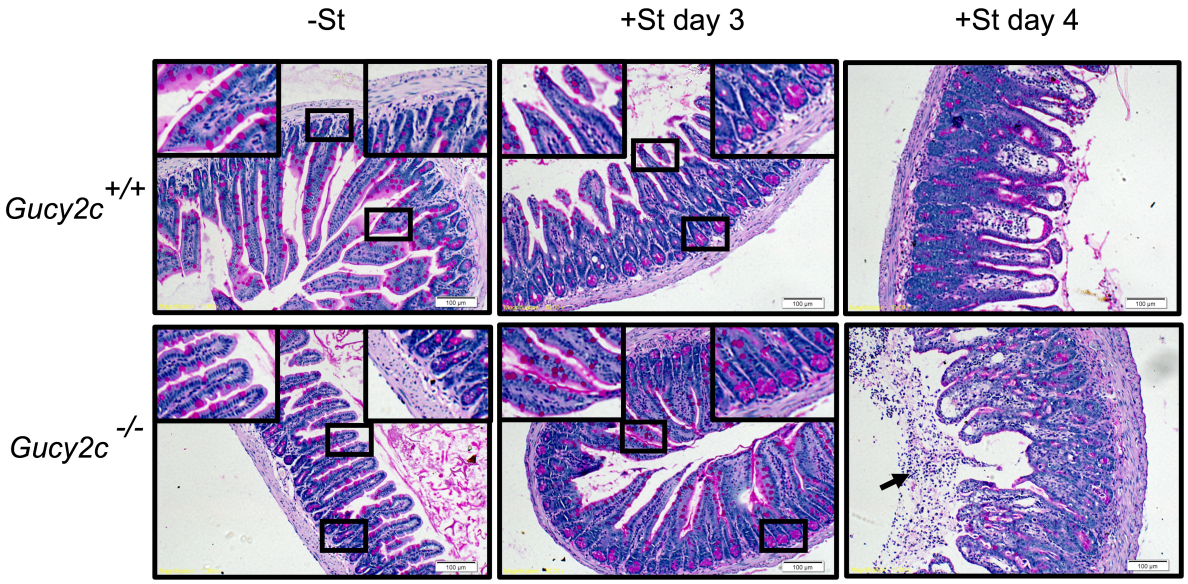
-St
+St day 3
+St day 4
Gucy2c+/+
Gucy2c-/-

c

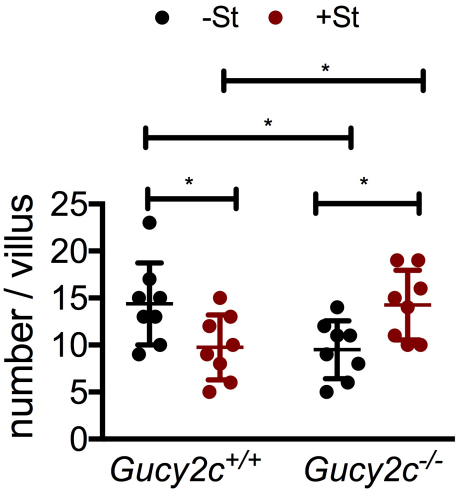
-St
+St
*
*
*
*
number / villus
25
20
15
10
5
0
Gucy2c+/+
Gucy2c-/-

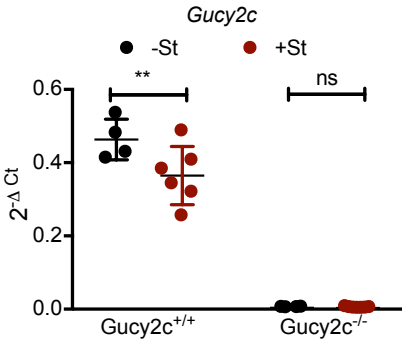
Gucy2c
-St
+St
**
ns
0.6
0.4
0.2
0.0
2-Δ Ct
Gucy2c+/+
Gucy2c-/-

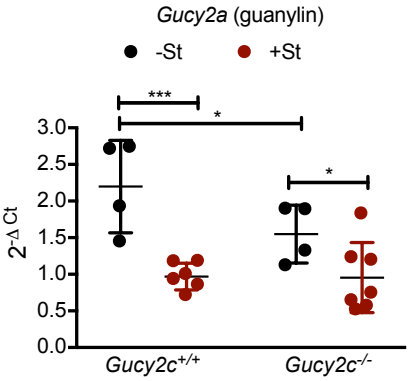
Gucy2a (guanylin)
-St
+St
***
*
*
3.0
2.5
2.0
1.5
1.0
0.5
0.0
2-Δ Ct
Gucy2c+/+
Gucy2c-/-

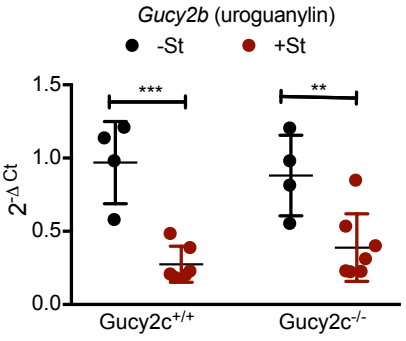
Gucy2b (uroguanylin)
-St
+St
***
**
1.5
1.0
0.5
0.0
2-Δ Ct
Gucy2c+/+
Gucy2c-/-

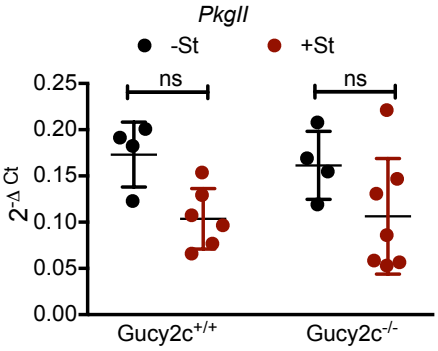
PkgII
-St
+St
ns
ns
0.25
0.20
0.15
0.10
0.05
0.00
2-Δ Ct
Gucy2c+/+
Gucy2c-/-

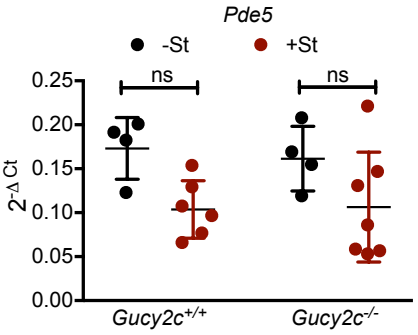
Pde5
-St
+St
ns
ns
0.25
0.20
0.15
0.10
0.05
0.00
2-Δ Ct
Gucy2c+/+
Gucy2c-/-

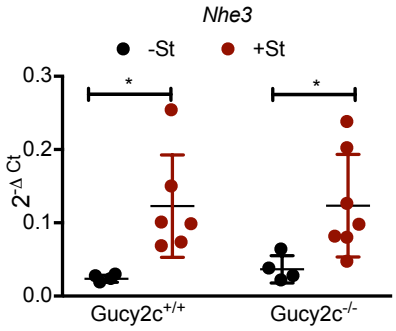
Nhe3
-St
+St
*
*
0.3
0.2
0.1
0.0
2-Δ Ct
Gucy2c+/+
Gucy2c-/-

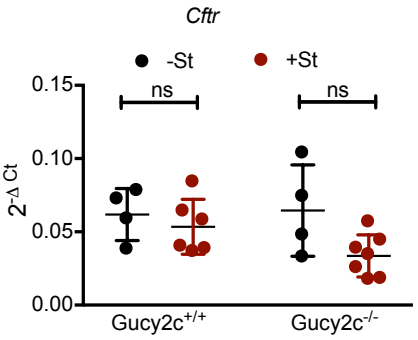
Cftr
-St
+St
ns
ns
0.15
0.10
0.05
0.00
2-Δ Ct
Gucy2c+/+
Gucy2c-/-

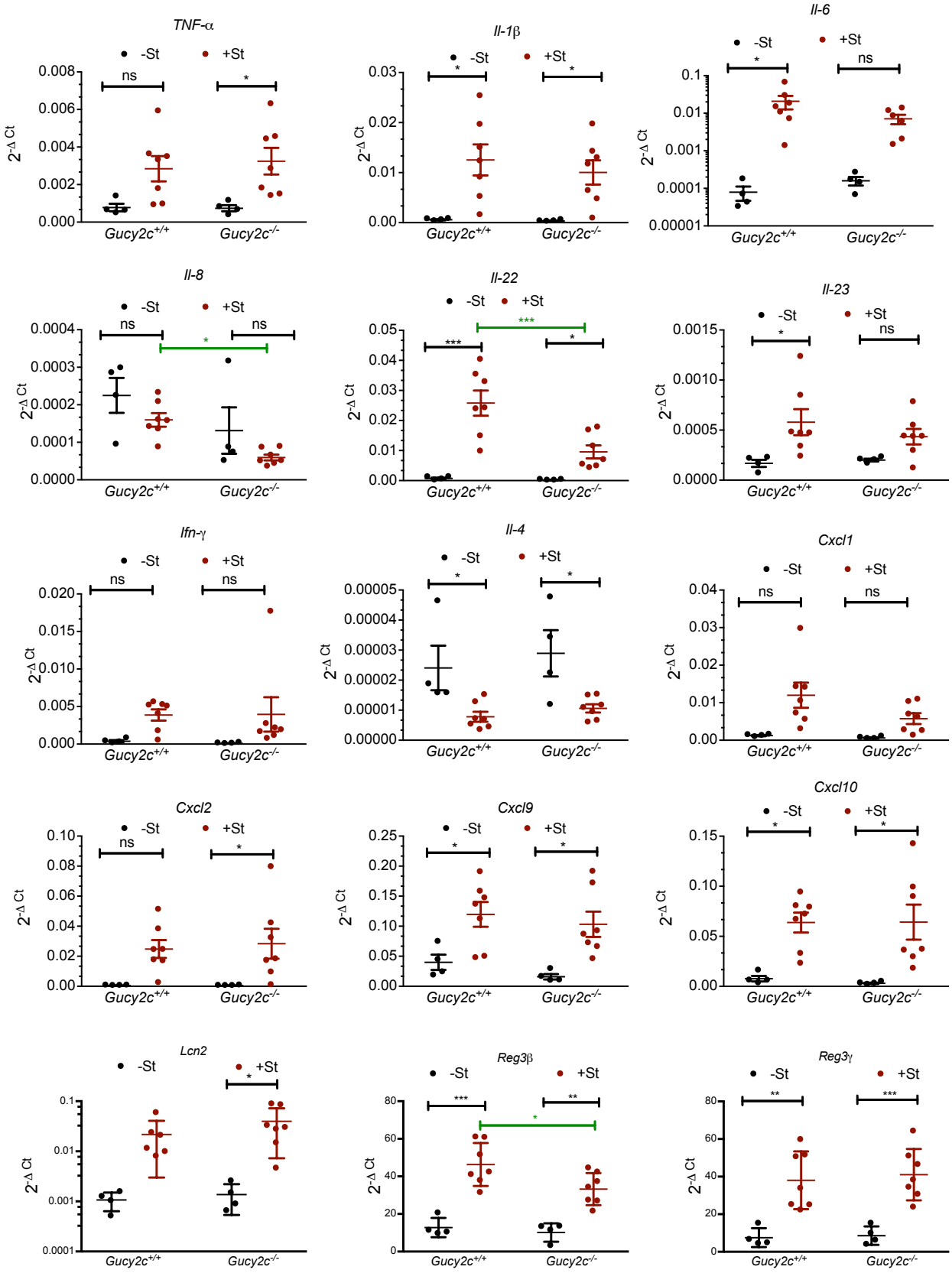
TNF-α
Il-1β
Il-6
Il-8
Il-22
Il-23
Ifn-γ
Il-4
Cxcl1
Cxcl2
Cxcl9
Cxcl10
Lcn2
Reg3β
Reg3γ
-St
+St
2^-Δ Ct
Gucy2c+/+
Gucy2c-/-
ns
*
**
***

a

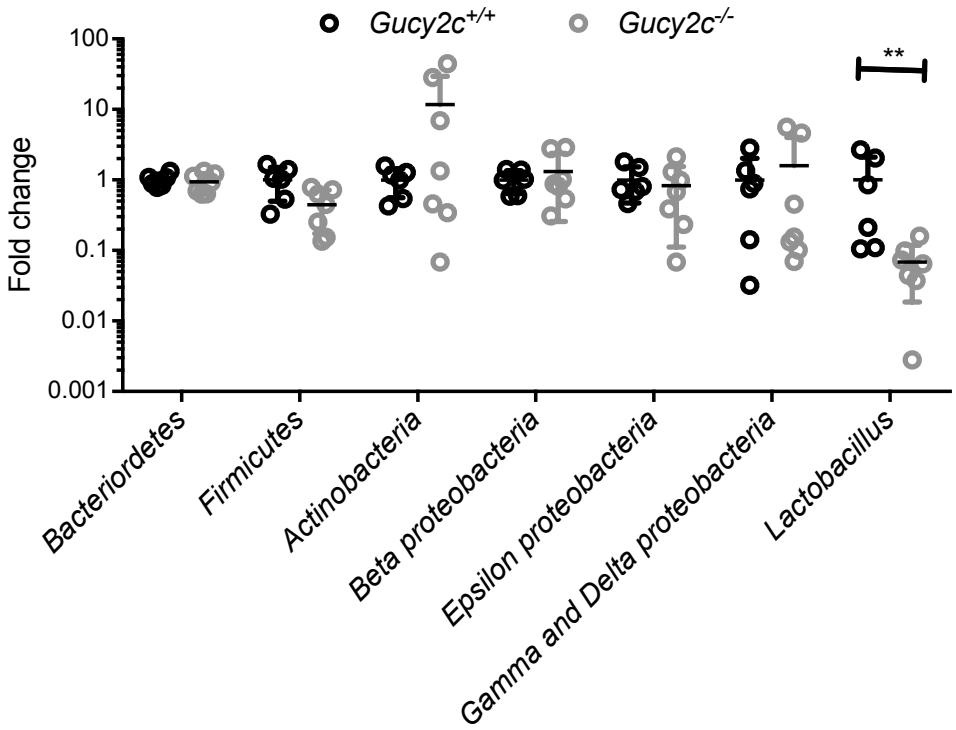
Gucy2c+/+
Gucy2c-/-
Fold change
100
10
1
0.1
0.01
0.001
**
Bacteriordetes
Firmicutes
Actinobacteria
Beta proteobacteria
Epsilon proteobacteria
Gamma and Delta proteobacteria
Lactobacillus

b

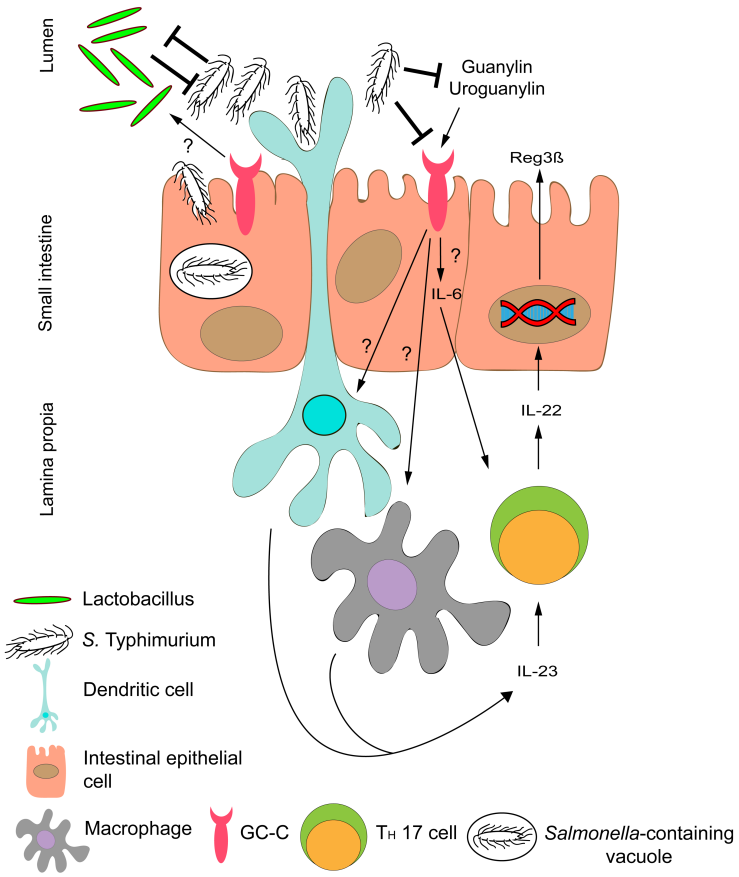
Lumen
Small intestine
Lamina propia
Guanylin
Uroguanylin
Reg3ß
?
IL-6
IL-22
IL-23
Lactobacillus
S. Typhimurium
Dendritic cell
Intestinal epithelial cell
Macrophage
GC-C
TH 17 cell
Salmonella-containing vacuole